Design, Synthesis, and Biological Evaluation of N'-Phenylhydrazides as Potential Antifungal Agents

Panpan Zhu , Jinshuo Zheng , Jin Yan , Zhaoxia Li , Xinyi Li , Huiling Geng *

Posted Date: 14 August 2023

doi: 10.20944/preprints202308.0996.v1

Keywords: N'-phenylhydrazide; antifungal activity; structure-activity relationship; antifungal mechanism

Article

Design, Synthesis, and Biological Evaluation of *N*′-Phenylhydrazides as Potential Antifungal Agents

Panpan Zhu [1,2], Jinshuo Zheng [1], Jin Yan [1], Zhaoxia Li [1], Xinyi Li [1] and Huiling Geng [1,2,*]

[1] College of Chemistry & Pharmacy, Northwest A&F University, Yangling 712100, Shaanxi, China; ppz@nwafu.edu.cn (P. Z.); zjs2021056749@nwafu.edu.cn (J. Z.); yanjin@nwafu.edu.cn (J. Y.); lizhaoxia@nwafu.edu.cn (Z. L.); lxy2022056825@nwafu.edu.cn (X. L.)

[2] Key Laboratory of Botanical Pesticide R & D in Shaanxi Province, Northwest A & F University, Yangling 712100, Shaanxi, China

* Correspondence: genghuiling@nwsuaf.edu.cn; Tel./Fax: +86-29-8709-2226

Abstract: Fifty-two kinds of *N*′-phenylhydrazides were successfully designed and synthesized. Their antifungal activity in vitro against five strains of *C. alb.* was evaluated. All prepared compounds owned varying degrees of activity and their MIC_{80}, TAI, and TSI values were calculated. The inhibitory activities of 27/52 compounds against fluconazole-resistant fungi *C. alb.* 4395 and *C. alb.* 5272 were much higher than those of fluconazole. The MIC_{80} values of 14/52 compounds against fluconazole-resistant fungus *C. alb.* 5122 were less than 4 μg/mL, so it was the most sensitive fungus (TSI_B = 12.0). **A**$_{11}$ showed the highest inhibitory activity against *C. alb.* SC5314, 4395, and 5272. The antifungal activities of **B**$_{14}$ and **D**$_5$ against four strains of fluconazole-resistant fungi were higher than those of fluconazole. The TAI values of **A**$_{11}$ (2.71), **B**$_{14}$ (2.13), and **D**$_5$ (2.25) are the highest. Further exploring the antifungal mechanism revealed that the fungus treated with compound **A**$_{11}$ produced free radicals and reactive oxygen species, and their mycelium morphology was damaged. In conclusion, the hydrazide scaffold showed potential in the development of antifungal lead compounds. Among them, **A**$_{11}$, **B**$_{14}$, and **D**$_5$ demonstrated particularly promising antifungal activity and hold potential as novel antifungal agents.

Keywords: *N*′-phenylhydrazide; antifungal activity; structure-activity relationship; antifungal mechanism

1. Introduction

The drug resistance of fungi shows a mounting trend, on account of the usage of various fungicides frequently for a long time, which made it more difficult to treat infections and led to severe illnesses and death [1]. The World Health Organization has reported the two worst threats to mankind's healthy, that is, the continuous increase of antimicrobial resistance for commercial antimicrobials against fungal infections, and the decreasing availability of effective therapies [2]. Fungal infections in humans are caused by *Candida*, *Aspergillus*, and *Cryptococcus* mainly [3]. *Candida* infection has emerged as a significant contributor to mortality among patients with malignant tumors, HIV, and organ transplants, which has resulted in severe consequences for the health of individuals worldwide [4].

As one of the four most common pathogens, *Candida albicans* (*C. alb.*) causes blood infections and is commonly found in the human gastrointestinal and reproductive tracts [5,6]. For instance, the monitoring results of invasive candidiasis in China show that *C. alb.* accounts for 44.9% among a total of 32 *Candida* species [7]. *C. alb*. is a dimorphic fungus that can grow in both yeast and hyphal forms [8]. In infection, its yeast form is more likely to disseminate in the blood, while the hyphal form penetrates tissues through the production of a fungal biofilm, evades phagocytic attack, and adheres to organs [9]. Approximately half of adults infect *C. alb.* in their oral and gastrointestinal microbiota, where it normally exists in a symbiotic relationship with the human body [10]. However, under conditions of a compromised immune system, it can overgrow and cause candidiasis [11]. Currently, inhibiting the transition between the two morphologies with drugs is an important way to reduce the

Preprints (www.preprints.org) | NOT PEER-REVIEWED | Posted: 14 August 2023 doi:10.20944/preprints202308.0996.v1

risk of *C. alb.* infection [12]. The results suggest that pathogenic fungi represent a significant and growing risk to human health. It is crucial to address fungal infections in the treatment of patients who have weakened immune systems [13].

Nowadays, various antifungal agents have been developed to cure candidiasis, which can be mainly categorized into four series including azoles, polyenes, echinocandins, and pyrimidines [14]. Among them, fluconazole (FLC) and caspofungin are the most commonly used in clinical (Figure 1) [15,16]. However, some strains of fungi have displayed resistance to these drugs, which results in treatment failure [17,18]. Additionally, these antifungal agents may cause side effects such as headache, fever, and liver damage [19], highlighting the urgent need for a new generation of fungicides [20]. Hydrazide is a common structural fragment found in active natural products and widely used medicines (Figure 2) [21]. Hydrazides not only exhibit various pharmacological activities such as inhibiting lipoxygenase, antiviral, antifungal, antioxidant, and anticancer effects but also own high inhibitory activity against phytopathogenic fungi and insects. Compound **1** displayed a high level of inhibition against lipoxygenase, with a potency of up to 93% observed at a concentration of 10 μM. [22]. A novel acylhydrazine derivative (compound **2**) with potent antiviral activity against the histone deacetylase (HDAC), its IC_{50} values against HDAC1, HDAC2, and HDAC3 were 0.5, 0.1, and 0.06 μM, respectively [23]. Compound **3** demonstrated a minimum inhibitory concentration range of 0.0156-0.125 mg/mL against three strains including *C. alb.*, *C. glabrata*, and *C. tropicalis* [24]. Compounds **4** and **5** exhibited potent antifungal activity against *C. alb.*, displaying MIC values of 12.5 μM [25]. Compound **6** owned modulative reactivity towards Cu (II)–amyloid β and free radicals. Furthermore, its ability to mitigate free radicals was found to be similar to that of trolox, which is a Vitamin E analyte [26]. Isoniazid was used clinically to treat depression and inspired the development of other drugs such as isocarboxazid (compound **7**), which had irreversible inhibitory effects on monoamine oxidase [27]. Compound **8** could effectively block the T-47D in the G2/M phase of the cell cycle [28]. Compound **9** could efficiently inhibit the growth of *Gibberella zeae*, *Fusium oxporum*, *Colletotrichum higgensianum*, and *Score-tiorum* and their inhibitory rates were 98%, 91%, 100%, and 99%, respectively, at a concentration of 25 μg/mL [29]. The LD_{50} value of compound **10** was 220 ng/insect against adult anopheles gambiae [30]. However, studies of *N*'-phenylhydrazides against the antifungal activity of *C. alb.* have not been reported.

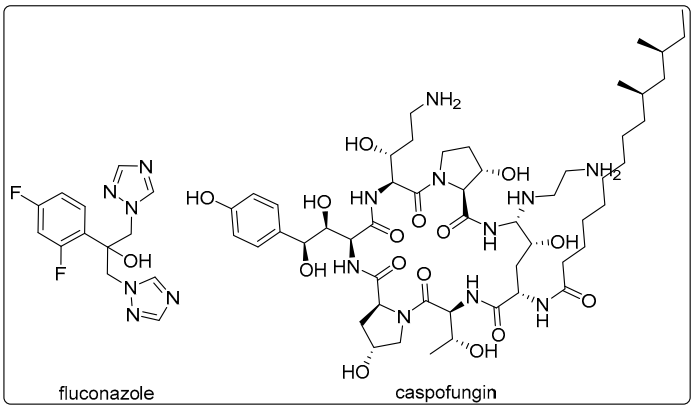

Figure 1. Commercial fungicides.

In this study, *N*'-phenylhydrazides were designed, synthesized, and structurally characterized. The antifungal activity against five strains of *C. alb.* was assessed via the broth microdilution (BMD) method, and initial structure-activity relationships (SARs) were established. To probe the antifungal mechanism, investigations were carried out involving free radical scavenging, confocal laser scanning microscopy (CLSM), and scanning electron microscopy (SEM).

Preprints (www.preprints.org) | NOT PEER-REVIEWED | Posted: 14 August 2023 doi:10.20944/preprints202308.0996.v1

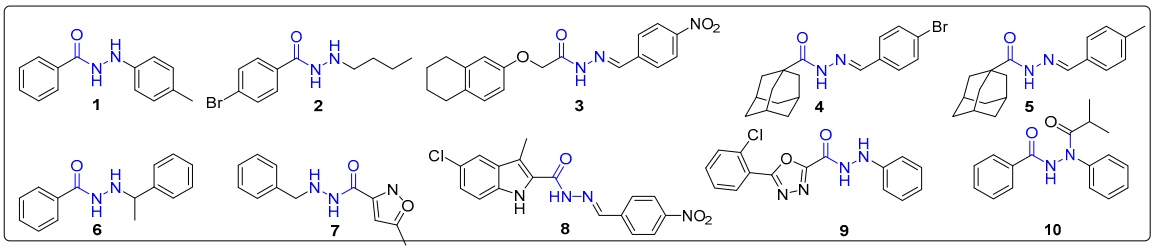

Figure 2. Hydrazides with biological activity.

2. Results and Discussion

2.1. Design and Synthesis of N′-Phenylhydrazides

The synthetic routes of the target compounds were shown in Figure 3. Substituted benzoyl chloride was synthesized by the acylation of substituted benzoic acid with $SOCl_2$. And a substitution reaction was occured between it and phenylhydrazine to gain series A compounds. At 0 °C, various substituted phenylhydrazines hydrochloride were achieved through the diazotization reactions. Then, series B compounds were got via the condensation reaction between phenylhydrazine hydrochloride with benzoic acid under EDCI and HOBt. The preparation of series C and D compounds was the condensation reaction between different kinds of carboxylic acids and phenylhydrazine hydrochloride.

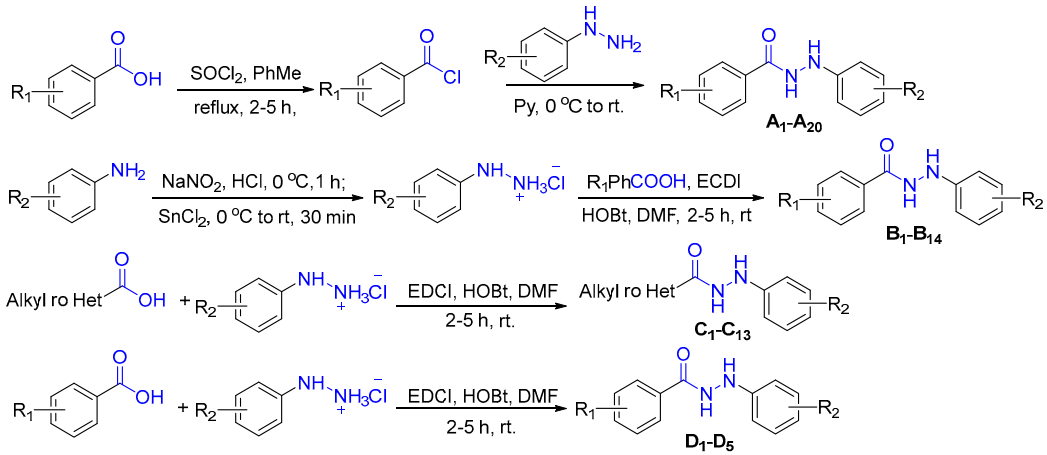

Compd.	R_1	R_2	Compd.	R_1	R_2	Compd.	R_1	R_2	Compd.	R_1	R_2
A_1	H	H	A_{14}	4-OMe	H	B_7	H	4-Me	C_6	2-naphthyl	H
A_2	2-F	H	A_{15}	4-Cl	H	B_8	H	4-OMe	C_7	2-thienyl	H
A_3	2-Me	H	A_{16}	4-CN	H	B_9	H	4-CN	C_8	3-thienyl	H
A_4	2-OMe	H	A_{17}	4-CF_3	H	B_{10}	H	4-CF_3	C_9	3-indolyl	H
A_5	2-Cl	H	A_{18}	4-Br	H	B_{11}	H	4-Cl	C_{10}	PhEt	H
A_6	2-CF_3	H	A_{19}	4-^{i}Pr	H	B_{12}	H	4-Br	C_{11}	PhPr	H
A_7	2-Me&4-Cl	H	A_{20}	4-NO_2	H	B_{13}	H	4-^{i}Pr	C_{12}	Et	H
A_8	3-F	H	B_1	H	2-Cl	B_{14}	H	4-F	C_{13}	amyl	H
A_9	3-Me	H	B_2	H	3,5-diCl	C_1	PhO	H	D_1	4-Cl	4-F
A_{10}	3-Cl	H	B_3	H	3-Cl	C_2	PhMe	H	D_2	3-F	3-Cl
A_{11}	3-CF_3	H	B_4	H	3-CF_3	C_3	2-furyl	H	D_3	3-CF_3	4-F
A_{12}	3,5-diF	H	B_5	H	3-Br	C_4	Cyclopropyl	H	D_4	3,5-diF	4-F
A_{13}	4-Me	H	B_6	H	4-I	C_5	1-naphthyl	H	D_5	3,5-diF	3-Cl

Figure 3. Synthesis of target compounds A_1-D_5.

A total of 52 *N*′-phenylhydrazides belonging to four different series were synthesized via concise and efficient methods in up to 96% yield. The structures of target *N*′-phenylhydrazides were identified by HRMS, ^{1}H NMR, and ^{13}C NMR spectra. It was discovered that five of them (**A_7**, **B_{13}**, **D_2**, **D_4**, and **D_5**) were unknown. The separated yields, melting points, and the data of HRMS, ^{1}H NMR, and ^{13}C NMR spectra of *N*′-phenylhydrazides were illustrated in the supporting information.

Preprints (www.preprints.org) | NOT PEER-REVIEWED | Posted: 14 August 2023 doi:10.20944/preprints202308.0996.v1

2.2. Evaluation of Antifungal Activity in Vitro

The in vitro antifungal activities of target candidates against five strains of *C. alb.* were screened at the concentration of 0.125, 0.25, 0.5, 1, 2, 4, 8, 16, 32, and 64 μg/mL through the broth microdilution (BMD) method. FLC was selected as the positive control. Based on the data of antifungal activity, their MIC_{80} values and total activity index (TAI) were calculated according to the formulas, $MIC_{80} = 10^{\log A + \log\frac{1}{N} \times \frac{a-80}{a-b}}$ and $TAI = \sum_1^n 1/\sqrt{MIC_{80}}$, respectively. The total susceptibility index (TSI) of every stain of fungus was evaluated as well. By analyzing MIC_{80} and TAI values, the preliminary SRAs were concluded. According to the standards of the Clinical Laboratory Standards Institute, when MIC_{80} values were distributed in ≤4 μg/mL, 8-16 μg/mL, and≥32 μg/mL, the corresponding compounds were classified as susceptible, intermediate, and resistant candidates, respectively. [31]. To evaluate the potency of the compounds with greater inhibitory activity, time-inhibition rate curves were depicted for seven compounds (**A_1**, **A_2**, **A_8**, **A_{11}**, **A_{12}**, **B_{14}**, and **C_8**) and their respective half-inhibitory time (IT_{50}) were calculated.

2.2.1. Antifungal Activity of Target Compounds

A total of fifty-two kinds of compounds were synthesized, their fungicidal activities in vitro were screened at the concentration in the range of 0.125-64 μg/mL against five strains of fungi, and their MIC_{80} values and TAI values were calculated (Table 1).

Table 1. MIC_{80} values (μg/mL) of target compounds against *C. alb.*

Compd.	R_1	R_2	*C. alb.***SC5314**	*C. alb.***4395**	*C. alb.***5122**	*C. alb.***5172**	*C. alb.***5272**	TAI
A_1	H	H	26.0	15.0	0.9	>64.0	>64.0	<1.76
A_2	2-F	H	13.0	4.1	8.5	6.7	12.1	1.79
A_3	2-Me	H	49.3	>64.0	13.3	21.2	53.0	N. A.[d]
A_4	2-OMe	H	14.7	31.0	5.7	7.8	6.4	1.61
A_5	2-Cl	H	25.3	52.5	10.8	13.8	13.0	1.19
A_6	2-CF_3	H	11.7	4.5	6.3	12.0	22.1	1.66
A_7	2-Me&4-Cl	H	26.0	>64.0	>64.0	23.4	63.0	N. A.
A_8	3-F	H	3.4	9.7	0.7	>64.0	27.0	N. A.
A_9	3-Me	H	25.3	61.4	10.5	14.7	17.8	1.13
A_{10}	3-Cl	H	6.9	6.6	15.0	12.3	59.0	1.44
A_{11}	3-CF_3	H	1.9	4.0	2.8	7.4	3.7	2.71
A_{12}	3,5-diF	H	3.6	25.0	1.6	>64.0	>64.0	N. A.
A_{13}	4-Me	H	13.9	31.0	5.0	14.6	27.0	1.35
A_{14}	4-OMe	H	5.9	32.0	1.5	>64.0	>64.0	N. A.
A_{15}	4-Cl	H	5.9	32.0	1.5	>64.0	>64.0	N. A.
A_{16}	4-CN	H	47.5	15.0	6.3	5.8[b]	7.2	1.6
A_{17}	4-CF_3	H	>64.0	15.0	4.6	9.6	9.3	N. A.
A_{18}	4-Br	H	24.4	>64.0	7.4	41.4	>64.0	N. A.
A_{19}	4-^{i}Pr	H	>64.0	61.3	>64.0	>64.0	13.5	N. A.
A_{20}	4-NO_2	H	6.7	16	0.8	>64.0	>64.0	N. A.
B_1	H	2-Cl	26.2	52.3	13.0	14.0	12.5	1.16
B_2	H	3,5-diCl	45.3	>64.0	32.2	45.0	>64.0	N. A.
B_3	H	3-Cl	6.9	19.0	0.7	>64.0	>64.0	N. A.
B_4	H	3-CF_3	>64.0	>64.0	31.5	58.6	>64.0	N. A.
B_5	H	3-Br	24.6	60.0	3.6	13.9	6.3	1.52
B_6	H	4-I	16.7	>64.0	31.8	30.0	19.0	N. A.
B_7	H	4-Me	13.4	32.0	21.5	25.0	13.2	1.14
B_8	H	4-OMe	9.2	22.0	0.8	>64.0	>64.0	N. A.
B_9	H	4-CN	>64.0	>64.0	>64.0	>64.0	62.6	N. A.
B_{10}	H	4-CF_3	>64.0	>64.0	>64.0	>64.0	>64.0	N. A.
B_{11}	H	4-Cl	10.7	12.3	4.8	7.1	57	1.56

Preprints (www.preprints.org) | NOT PEER-REVIEWED | Posted: 14 August 2023 doi:10.20944/preprints202308.0996.v1

B12	H	4-Br	47.5	14.7	50.4	30	13.1	1.00
B13	H	4-^{i}Pr	14.3	>64.0	21.0	52.7	>64.0	N. A.
B14	H	4-F	12.2	4.0	3.5	3.3	14.7	2.13
C1	PhO	H	31.7	14.3	11	6.7	7.2	1.50
C2	PhMe	H	3.4	42	1.7	>64	>64	N. A.
C3	2-furyl	H	17.5	45.8	2.7	7.3	13	1.64
C4	Cyclopropyl	H	58.9	8.9	7.7	3.9	3.8	1.85
C5	1-naphthyl	H	>64.0	>64.0	62.0	>64.0	>64.0	N. A.
C6	2-naphthyl	H	14.6	>64.0	51.8	58.7	>64.0	N. A.
C7	2-thienyl	H	14.2	60.0	7.0	16.5	42.0	1.17
C8	3-thienyl	H	13.9	22.6	11.6	14.7	>64.0	N. A.
C9	3-indolyl	H	>64.0	>64.0	>64.0	1.4	>64.0	N. A.
C10	PhEt	H	51.8	16.1	15.0	>64.0	11.0	N. A.
C11	PhPr	H	>64.0	>64.0	22.8	>64.0	15.2	N. A.
C12	Et	H	>64.0	>64.0	13.8	>64.0	12.1	N. A.
C13	amyl	H	>64.0	42.6	34.4	>64.0	28.5	N. A.
D1	4-Cl	4-F	12.2	5.5	6.4	3.7	29.5	1.81
D2	3-F	3-Cl	>64.0	13.8	9.6	>64.0	7.6	N. A.
D3	3-CF_3	4-F	63.6	>64	3.8	>64.0	7.6	N. A.
D4	3,5-diF	4-F	30.4	13.5	6.3	>64.0	7.6	N. A.
D5	3,5-diF	3-Cl	64	29.3	2.2	2.7	2.4	2.25
	FLC		1.8[a]	>128.0	58.0	>64.0	>128.0	<1.19[c]

* a: red color refers to susceptible; b: green color refers to the highest activity; c: due to FLC's MIC_{80} values being greater than 128 μg/mL for *C. alb.* 4395, thus, the TAI value of FLC was recorded as<1.19; d: N. A. means that their TAI values are not available.

All target compounds displayed definite inhibitory activities against the five test fungi. In terms of series A compounds, **A11** held the best inhibitory activity against *C. alb.* SC5314, 4395, and 5272 and the corresponding MIC_{80} value was 1.9, 4.0, and 3.7μg/mL, respectively. Thus, **A11** owned the highest TAI value (2.71). **A8** (MIC_{80} = 0.7 μg/mL) showed the best inhibitory activity against *C. alb.* 5122. As far as the *C. alb.* 5172 was concerned, **A16** (MIC_{80} = 5.8 μg/mL) displayed the best inhibitory activity against it.

As far as series B compounds were concerned, **B3** (MIC_{80} = 6.9 μg/mL) held the most effictive antifungal activity against *C. alb.* SC5314. **B14** had the most potent inhibitory activity against *C. alb.* 4395 and 5172 and the corresponding MIC_{80} values were 4.0 and 3.3 μg/mL, respectively. It also owned the highest TAI value (2.13). As far as the *C. alb.* 5122 was concerned, **B3** (MIC_{80} = 0.7 μg/mL) displayed the best inhibitory activity against it. **B5** (MIC_{80} = 6.3 μg/mL) showed the best inhibitory activity against *C. alb.* 5272.

As for series C compounds, **C2** had the best inhibitory activity against *C. alb.* SC5314 and 5122 and the corresponding MIC_{80} values were 3.4 and 1.7 μg/mL, respectively. As far as the *C. alb.* 4395 and 5272 were concerned, **C4** displayed the highest inhibitory activity against them and the corresponding MIC_{80} values were 8.9 and 3.8 μg/mL, respectively. **C4** owned the highest TAI value (1.85). **C9** (MIC_{80} = 1.4 μg/mL) showed the most powerfully antifungal activity against *C. alb.* 5172.

With respect to series D compounds, **D2** exhibited the most potent antifungal activity against *C. alb.* SC5314 and 4395 with MIC_{80} values of 12.2 and 5.5 μg/mL, respectively. As far as the *C. alb.*5122, 5172, and 5272 were concerned, **D5** displayed the best inhibitory activity against them and the corresponding MIC_{80} values were 2.2, 2.7, and 2.4μg/mL, respectively. Hence, **D5** owned the highest TAI value (2.25).

2.2.2. The Inhibitory Efficiency of Compounds with Higher Activity

In order to evaluate the inhibitory potential of the compounds exhibiting higher activity, time-inhibition rate curves were depicted for seven compounds (**A1**, **A2**, **A8**, **A11**, **A12**, **B14**, and **C8**) at the

Preprints (www.preprints.org) | NOT PEER-REVIEWED | Posted: 14 August 2023 doi:10.20944/preprints202308.0996.v1

concentration of 3.2 μg/mL against *C. alb.* SC5314 and their half-inhibitory times (IT_{50}) were calculated (Figures 4 and 5).

The time-inhibition rate curve of FLC showed a relatively smooth overall trend, whereas those of the seven tested compounds exhibited a steep rise in the inhibition rate during the 0-10 hours period and was followed by a gradual flattening after 20 hours. According to calculations, the IT_{50} value of FLC was 14.1 h. In contrast, the IT_{50} values of all seven tested compounds were less than 7.5 h. Compound **A**$_{11}$, in particular, achieved the lowest IT_{50} value (1.4 h). Thus, this class of compounds held a more efficient antifungal efficacy, which might be attributed to their simple structure making them easy to enter fungal cells.

2.2.3. The Analysis of Preliminary SARs

In this study, the compounds with TAI values ≥1.19 were defined as susceptible compounds. When 25% of *N'*-phenylhydrazides owned MIC_{80} values ≤4 μg/mL against the fungi, the fungi were defined as sensitive ones. Sixteen susceptible compounds and one sensitive fungus, *C. alb.* 5122 were screened.

According to the above data, the TAI values of twenty-one compounds (**A**$_2$, **A**$_4$, **A**$_5$, **A**$_6$, **A**$_9$, **A**$_{10}$, **A**$_{11}$, **A**$_{13}$, **A**$_{16}$, **B**$_1$, **B**$_5$, **B**$_7$, **B**$_{10}$, **B**$_{11}$, **B**$_{14}$, **C**$_1$, **C**$_3$, **C**$_4$, **C**$_7$, **D**$_1$, and **D**$_5$) with MIC_{80} ≤64 μg/mL were calculated according to the formula, $TAI = \sum_1^n 1/\sqrt{MIC_{80}}$, which reflected the antifungal activity of the compounds, and the larger the index, the higher the antifungal activity of the compound [32].

The total susceptibility index (TSI) of the fungi were calculated according to the formula, $TSI = \sum_1^n 1/\sqrt{MIC_{80}}$, which reflects the sensitivity of every strain of *C. alb.*, and the greater the index, the more sensitive the fungus is to these compounds (Table 2) [32].

Standard *C. alb.* SC5314 exhibited a high degree of sensitivity to FLC (TSI = 14.8). For series A and B compounds, the most sensitive fungus was *C. alb.* 5122, the TSI values were 11.6 and 12.0, respectively. *C. alb* 5172 showed the highest sensitivity to series C and D compounds, the TSI values were 7.8 and 11.2, respectively. Thus, *C. alb.* 5122 was a sensitive fungus.

The MIC_{80} and TAI values obtained allowed a preliminary evaluation of SARs. Contrast with **A**$_1$ to obtain the general trends.

First, the introduction of a chlorine atom to the *ortho*-, *meta*-, or *para*-position of the carbonyl side benzene ring was able to sharply enhance the antifungal activity against all or most of the fungi (**A**$_5$, **A**$_{10}$, and **A**$_{15}$). A similar case was observed for *ortho*-/*meta*-F, *para*-Br and *meta*-/*para*-CF_3 substituted compounds (**A**$_2$, **A**$_8$, **A**$_6$, **A**$_{11}$, and **A**$_{17}$). The more electron-withdrawing groups on ring A, the better the antifungal activity of the corresponding compounds (**A**$_{12}$>**A**$_7$).

Second, the introduction of nine substituents, identical to those present in the series A compounds, onto the phenyl ring of hydrazine side resulted in compounds with inferior antifungal activity compared to the series A compounds. Among the tested compounds, those with *para*-CH_3, *para*-Cl, and *para*-F substituents (**B**$_7$, **B**$_{11}$, and **B**$_{14}$) exhibited higher fungicide activities compared to *ortho*-Cl and *meta*-Br substitutes (**B**$_1$ and **B**$_5$).

Preprints (www.preprints.org) | NOT PEER-REVIEWED | Posted: 14 August 2023 doi:10.20944/preprints202308.0996.v1

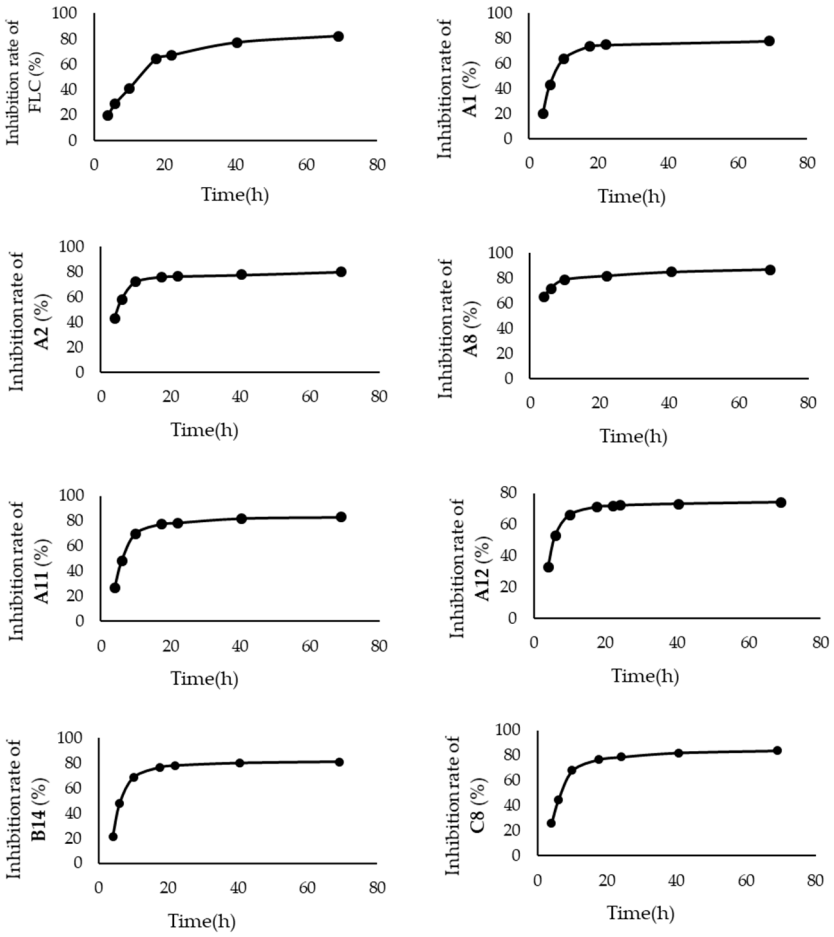

Figure 4. Curves of time-inhibition rate for each compound.

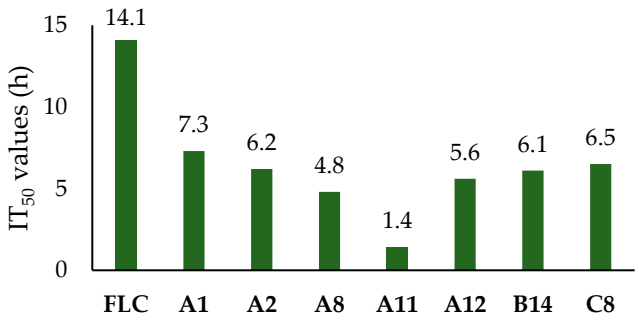

Figure 5. The IT_{50} values of the seven compounds (h).

Third, the fungicide activity was also influenced by the various heterocycles and alkyl groups. **C**$_4$ with cyclopropyl significantly improved the fungicide activities toward *C. alb.* 5172 and 5272. However, the activities were cut down by the naphthyl group consumedly. A similar case was found for **C**$_3$, **C**$_7$, and **C**$_8$ with polar heterocyclic groups (thienyl and furan), which were less effective than **A**$_1$. The short-chain alkane counterparts (**C**$_{12}$) possessed better activities against five strains of fungi than their long-chain alkane counterparts (**C**$_{13}$). The longer the carbon chain between the benzene ring and the carbonyl group, the lower the antifungal activity of the corresponding compounds (**C**$_{11}$<**C**$_{10}$<**C**$_2$).

Preprints (www.preprints.org) | NOT PEER-REVIEWED | Posted: 14 August 2023 doi:10.20944/preprints202308.0996.v1

Table 2. TSI values of the specific fungus to all target compounds.

Compd.	SC5314	4395	5122	5172	5272
A	6.4	5.4	11.6	5.8	5.2
B	5.0	4.8	12.0	4.8	5.0
C	5.0	4.2	6.4	7.8	5.8
D	3.4	5.8	9.2	11.2	7.6
FLC	14.8	<1.8[a]	2.6	<2.6	<1.8[a]

*a: the MIC_{80} values of FLC for *C. alb.* 4395 and 5272 were greater than 128 μg/mL, so their TSI values were recorded as<1.8.

Last, combining the pharmacophores of ring A (-F, -Cl, and $-CF_3$) and B (-F and -Cl) sharply enhanced the antifungal activity of series D compounds. However, their antifungal activity still did not reach the level of **A11**.

2.3. The Investigation of the Antifungal Mechanism

In this research, *C. alb.* SC5314 was chosen as the tested fungi, and **A11** with the highest TAI (2.71) value was used as the tested compound.

2.3.1. Assay of Free Radical Scavenging

In this assay, glutathione was selected as the free radical scavenger. With an increase in the concentration of glutathione, the inhibition rate of **A11** against *C. alb.* SC5314 decreased continuously. When the concentration of glutathione reached 1600 μg/mL, the antifungal effect of **A11** was essentially disappeared (Figure 6).

At concentrations of 1600, 800, and 400 μg/mL, glutathione exhibited low inhibitory effects on the growth of standard *C. alb.* SC5314 and the inhibition rate of **A11** remained consistently stable at around 95%. At the time of the concentrations of glutathione increased, the inhibitory effect of **A11** reduced. In the event of the concentration of glutathione was at 400 μg/mL, the inhibition rate of **A11** decreased from 94.7% to 18.4%. On the occasion that the concentration of glutathione was raised to 800-1600 μg/mL, the inhibition rate of **A11** dropped to below 20%, similar to the inhibition rate observed when glutathione was used alone. This indicated that **A11** produced free radicals during the metabolism process within fungal cells.

2.3.2. Production of ROS

To monitor cellular redox processes, the common oxidative stress indicator DCFH-DA was utilized. As shown in Figure 7, treatment with **A11** resulted in a significantly higher fluorescence intensity of DCFH-DA (Figure 7A–C) as compared to the control groups (Figure 7D). These results suggested that **A11** could impair mitochondrial function and increase the production of large numbers of ROS in *C. alb.* SC5314.

2.3.3. Effects of **A11** on Hyphal Morphology

The impact of **A11** on the hyphal morphology against *C. alb.* SC5314 was observed by SEM. In Figure 8A–F, significant morphological changes in the filamentous form of *C. alb.* were observed after treatment with 20 μg/mL of **A11** compared to the control group. The untreated hyphae exhibited dispersed, regular, plump, uniform, and smooth surfaces (Figure 8A,B). In contrast, the treated hyphae appeared shriveled, distorted, with rough surfaces and displayed folding, wrinkling, and invagination (Figure 8C,D). Figure F depicted an abnormal transition of the fungus from the yeast form to the filamentous form.

According to the electron microscopy observations, the integrity of mycelia was damged by **A11**. The disruptive effect of **A11** on hyphal morphology was the main reason for its inhibitory activity.

Preprints (www.preprints.org) | NOT PEER-REVIEWED | Posted: 14 August 2023 doi:10.20944/preprints202308.0996.v1

2.3.4. Preliminary Antifungal Mechanisms

Based on the research results in 2.3.1 and 2.3.2, the metabolic processes of **A11** within the cell could be preliminarily analyzed. Firstly, **A11** was hydrolyzed by fungal amidase to generate phenylhydrazine. In the structure of hydrazine (H_2N-NH_2), the lone pairs of electrons on the nitrogen atoms repelled each other strongly and led to the reducibility of phenyl hydrazides. Then, under the action of P450, phenyl hydrazine was oxidized to diazo compounds and then released nitrogen gas and generated free radicals. Their reducibility could lead to the reduction of oxygen within cells, forming reactive oxygen species (ROS) as well such as superoxide anions and hydroxyl radicals. Excessive ROS and free radicals disrupted the normal physiological processes of the fungus and subsequently affected the hyphal morphology of the fungi (Figure 9). This antifungal mechanism was similar to previously reported [33].

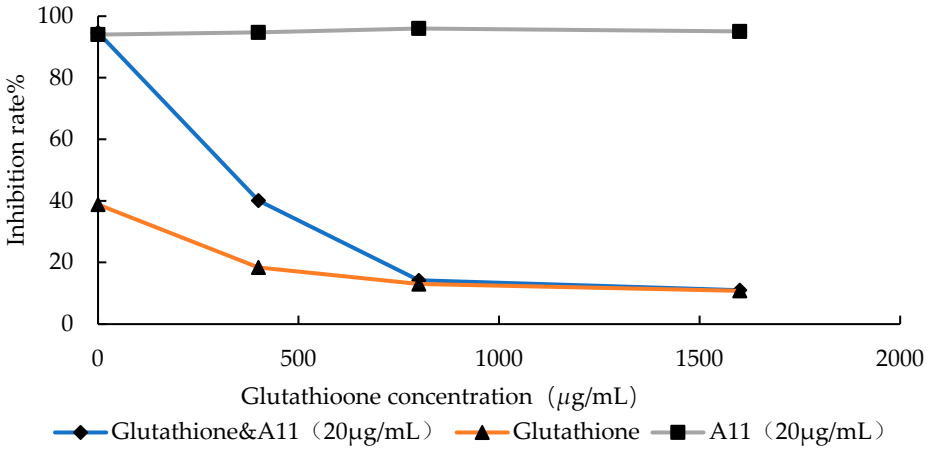

Figure 6. Effect of glutathione on the inhibition rate.

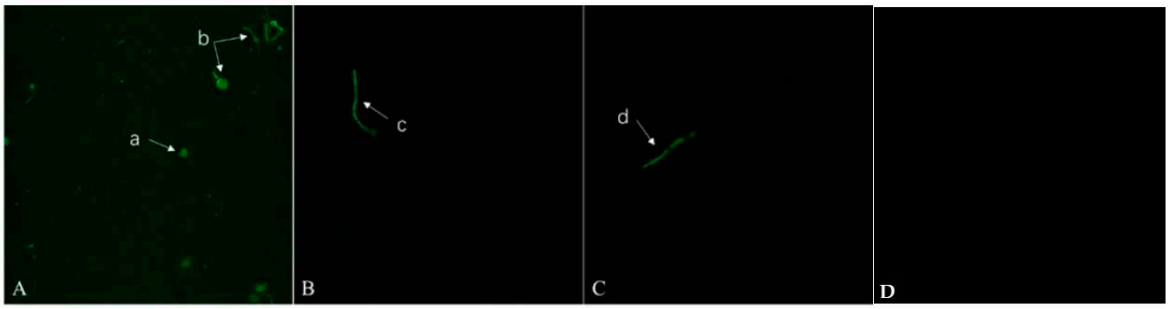

* a, the yeast form of *C. alb.*; b, the budding state of *C. alb.*; c and d, the filamentous form of *C. alb.*

Figure 7. Effects of compound **A11** on the ROS of *C. alb.* SC5314.

The different degrees of inhibition of *C. alb*. by target compounds stemmed from two factors. Firstly, their antifungal activity was affected by the rate of free radical production. The hydrolysis of amide bonds was the first step in the metabolism of *N*'-phenylhydrazines and was also a necessary condition for the formation of free radicals. The electron cloud density of the carbonyl group can be reduced and the hydrolysis of the amide bond can be promoted when the electron absorbing group was introduced to the substituted benzoic acid, thus the formation rate of the corresponding free radical was faster. For example, the *ortho*-fluoride, *ortho*-trifluoromethyl, *meta*-chlorine, *meta*-trifluoromethyl, and *para*-cyano substituted compounds (**A2**, **A6**, **A10**, **A11**, and **A16**) had higher antifungal activity compared to the *ortho*-, *meta*- or *para*-methyl and *para*-methoxy substituted ones (**A2**, **A9**, **A13**, and **A14**). The different substituents affected the affinity between the corresponding compounds and hydrolase and the hydrolysis rate and antifungal activity of the compounds.

Preprints (www.preprints.org) | NOT PEER-REVIEWED | Posted: 14 August 2023 doi:10.20944/preprints202308.0996.v1

Secondly, their antifungal activity depend on the stability of the generated free radicals, and the poorer the stability of the free radicals, the higher the antifungal activity of the compound. The electron-withdrawing group reduced the electron cloud density of the benzene ring thereby reducing the stability of substituted phenylhydrazine. For example, compounds substituted with *meta* or *para* halogen atoms (**B**$_5$, **B**$_{11}$, **B**$_{12}$, and **B**$_{14}$) exhibited higher activity compared to compounds substituted with *para* methyl groups (**B**$_7$).

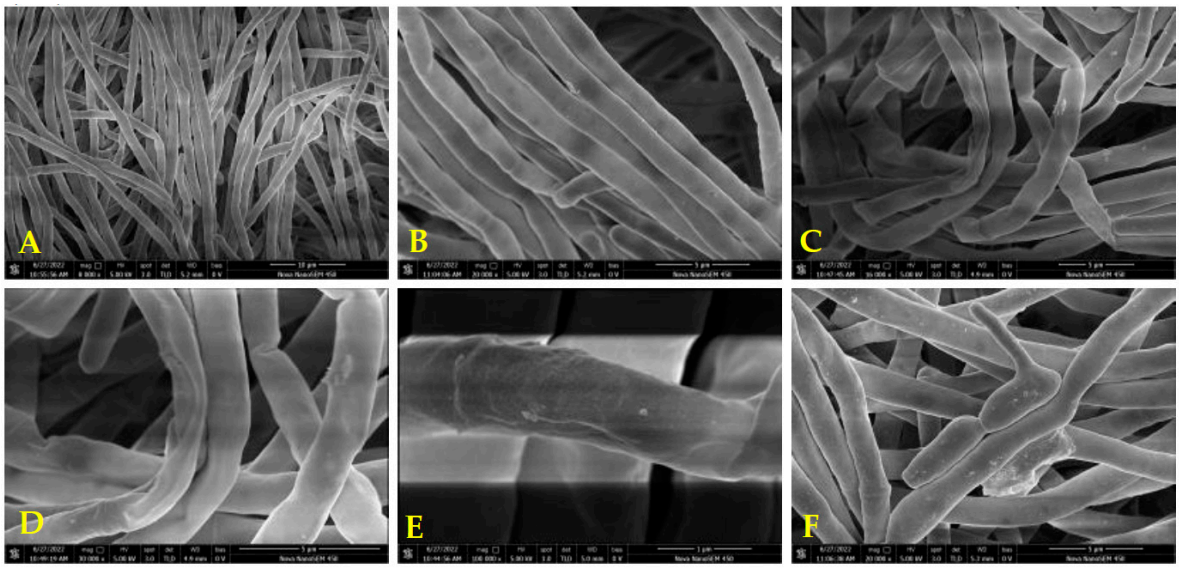

Figure 8. Microstructure of *C. alb.* SC5314 under SEM.

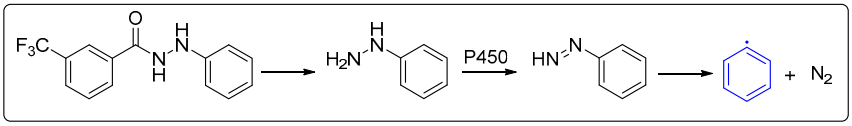

Figure 9. The metabolic process of **A**$_{11}$ in cells.

The pathogenicity of *C. alb.* is closely associated with the formation of hyphae, which is also an important factor in the formation of biofilms [34]. Typically, the filamentous form of *C. alb.* exhibits greater pathogenicity compared to the yeast form [35]. Under normal growth conditions, the hyphae surface appears uniform, plump, and smooth without any folds or wrinkles. In the pathological state, the microscopic appearance of the fungal hyphae exhibits signs of invagination and folding [36]. According to Figure 8, it can be observed that the treatment of *C. alb.* with compound **A**$_{11}$ resulted in an abnormal morphology of the hyphae. This indicated that compound **A**$_{11}$ exhibited a certain degree of inhibition on the formation and growth process of *C. alb.* hyphae. **A**$_{11}$ undergone metabolism within the fungal cells and led to the generation of free radicals and ROS disrupted the normal physiological processes of the fungus, and subsequently damaged its hyphal morphology. Next, in vivo antifungal activity and cytotoxicity assay tests will be carried out.

3. Materials and Methods

3.1. Materials

Substituted benzoic acid, substituted phenyl, substituted phenyl hydrazine hydrochloride, 1-Ethyl-3-(3-dimethylaminopropyl) carbodiimide hydrochloride (EDCI), 1-Hydroxybenzotriazole (HOBt), dried *N*, *N*-Dimethylformamide (DMF), pyridine, heterocyclic carboxylic acids, alkyl carboxylic acid, phenylhydrazine, fluconazole, and dimethyl sulfoxide (DMSO) were all purchased from Adamas Reagent Co. Ltd. (Shanghai, China). Other analytical pure reagents and solvents were bought from local companies. And before using a number of reagents were purified by standard

 doi:10.20944/preprints202308.0996.v1

procedures. Without other explicit direction, water was redistilled and ions were removed before use.

Standard *C. alb.* SC5314 was donated by Professor Dazhi Zhang of the Second Military Medical University. FLC-resistant fungi *C. alb.* 4935, 5122, 5172, and 5272 were donated by Professor Changzhong Wang of Anhui University of Chinese Medicine. At 30 °C, the tested fungi were cultured for 48 h on the reasoner's 2A (R2A) agar plates. The dilution of suspension was made with RPMI medium 1640, a volume of 1 mL of these suspensions contained 1×104–1×105 colony forming unit. The Tested compounds were diluted at the concentration of 8 μg/mL with DMSO.

Making use of a mixture of petroleum ether (PE) and ethyl acetate (EtOAc) as the mobile agent and thin-layer chromatography (TLC) using GF_{254} silica gel to monitor the progress of the reactions. An XT-4 micro melting point instrument was used to measure the melting point of every target compound. A Bruker Advance neo spectrometer (400 MHz) was applied to obtain the ^{1}H NMR and ^{13}C NMR spectrum of every synthesized chemical. Chemical shifts (δ values) and coupling constants (J values) were presented in ppm and Hz, respectively. The high-resolution mass spectra (HRMS) was took advantaged of to characterize every unknown compound. On a mass spectrometer (Thermo Scientific LTQ Orbitrap XL) the positive ion mass spectra of the samples were gained.

Thin-layer chromatography (TLC) precoated GF254 silica gel was employed to monitor the progression of each reaction. The mobile phase consisted of a mixed solution of petroleum ether (PE) and ethyl acetate (EtOAc). The melting points of every target compound was measured using an XT-4 micro melting point instrument. ^{1}H NMR and ^{13}C NMR spectra of all target compounds were obtained at 400 MHz using a Bruker Advance neo spectrometer. Chemical shifts (δ values) were reported in ppm while coupling constants (J values) were presented in Hz. Additionally, high-resolution mass spectra (HRMS) were performed to further characterize all unknown products. Positive ion mass spectrometry of the sample was acquired using a Thermo Scientific LTQ Orbitrap XL instrument.

3.2. The synthetic procedure

3.2.1. Synthesis of Substituted Phenylhydrazine Hydrochloride

Added $NaNO_2$ (1.90 g, 27.5 mmol,1.1 equiv.) to a solution of substituted aniline (2.33 g, 25 mmol, 1 equiv.) in hydrochloric acid (60 mL, 20%, V/V), at 0°C and stirred the reaction mixture at this temperature for 1 h. Then added the SnCl2 (9.48 g, 2 equiv., 50mmol) and stirred the mixture for 2 h at room temperature. The precipitate was filtered and washed with brine and Et_2O, and dried in vacuo at 40°C overnight [37].

3.2.2. Synthesis of N′-Phenylhydrazides

EDCI (8.8 mmol, 1.1 equiv.) and HOBt (8.8mmol, 1.1 equiv.) were added to a solution of carboxylic acid (8.0 mmol, 1 equiv.) in DMF (20 mL), then phenylhydrazine hydrochloride was added and the reaction mixture was stirred at ambient temperature under nitrogen atmosphere for 3 h, TLC detection. The reaction mixture was poured into H_2O (300 mL), filtrated, and recrystallized by ethanol to give the desired light yellow or brownish-yellow product [29].

3.3. Antifungal Activity In Vitro

3.3.1. Determination of MIC_{80} value

The antifungal activities in vitro of target compounds against five stains of fungi were determined via the BMD method with assays in 96-well plates. FLC was selected as the positive control [31].

To prepare the stock solutions of the tested compounds, they were dissolved in 100% DMSO with a concentration of 0.8 mg/mL. Before the assay the solutions were diluted to the concentration of 8.0 μg/mL with RPMI medium 1640. The final concentrations of tested compounds were 64, 32, 16, 8, 4, 2, 1, 0.5, 0.25, and 0.125μg/mL. After inoculation, the plates were incubated at 30 °C for 24 h. The

Preprints (www.preprints.org) | NOT PEER-REVIEWED | Posted: 14 August 2023 doi:10.20944/preprints202308.0996.v1

absorbance of each well was scanned at a wavelength of 625 nm via an ELISA reader, and the inhibition rate was calculated.

$$\text{Inhibition rate (\%)} = [(A_P - A_D)/ (A_P - A_N)] \times 100\% \quad (1)$$

Where A_P is the absorbance of positive control wells, A_D is the absorbance of drug wells and A_N is the absorbance of negative control wells.

The MIC_{80} values were the concentration of tested compounds when the inhibition rate was at 80%. A curve was plotted with the logarithm of the concentration as the horizontal axis and the inhibition rate as the vertical axis, and the MIC_{80} was calculated.

$$MIC_{80}=10^{\log A+\log\frac{1}{N}\times\frac{a-80}{a-b}} \quad (2)$$

Among them, A refers to the corresponding minimum concentration in the aforementioned gradient concentrations when the inhibition rate is just above 80%. a is the inhibition rate at concentration A, b is the inhibition rate just below a, and N represents the dilution factor.

3.3.2. Time-Inhibition Rate Curves

6.4 mg of the tested compound was dissolved in 0.5 mL of DMSO, then added RPMI medium 1640 to obtain a drug solution with a concentration of 3.2 μg/mL. The specific procedures are the same as those described in section 3.3.1. The absorbances were recorded at 0 h, 4 h, 6 h, 10 h, 17.5 h, 22 h, 24 h, 40.5 h, and 70 h, respectively. Every test was conducted three times. The time-inhibition rate curves were plotted by origin software with the time represented on the x-axis and the corresponding inhibition rate on the y-axis.

3.4. The Investigation of the Antifungal Mechanism

3.4.1. Scavenging of Free Radical Generated from A_{11}

The impact of **A_{11}** on the emergence of free radical of *C. alb.* SC5314 was evaluated. Glutathione with gradient concentrations (400, 800, and 1600 μg/mL) was set as a control group to exclude its effect on fungal growth. **A_{11}** at the concentration of 20 μg/mL had pretty antifungal activity, and its inhibition rate against *C. alb.* SC5314 was close to 100%. **A_{11}** was added to gradient concentrations (400, 800, and 1600 μg/mL) of glutathione and achieved a concentration of **A_{11}** of 20 μg/mL. As shown in 3.3.1., the assay should be followed.

3.4.2. Production of ROS

The influence of **A_{11}** on the generation of ROS of *C. alb.* SC5314 was ascertained as previously described [38]. DCFH-DA (2',7'-dichlorodihydrofluorescein diacetate, 40 μM, 0.5mL) was used to stain the hyphal tips of the fungal mycelium, followed by incubation in the dark at 25°C for 20 minutes and cleansed with PBS twice, each time for 5 minutes. At an excitation and emission wavelength of 488 nm and 525 nm, respectively, the fluorescence images were observed and captured before and after stimulation by CLSM (LEICA TCS SP8). Images were stored on a computer for further processing and analysis.

3.4.3. Analysis of the Mycelial Morphology

By SEM, the mycelial morphology of *C. alb.* SC5314 was observed according to the reported method [38]. Compound **A_{11}** (TAI = 2.71) and standard *C. alb.* SC5314 was chosen as the tested specimen and fungus, respectively.

The fungi were cultured in a thermostatic shaker at 37 °C and 200 rpm for a period of 8 to 24 hours. Subsequently, they were soaked in a 4% glutaraldehyde solution for a duration of 4 hours. Following this, the fungi were washed three times using a 0.1 mol/L PBS solution with a pH of 7.2. To initiate dehydration, the fungi were exposed to a series of ethanol concentrations including 30%, 50%, 70%, 80%, and 90% (v/v). Thereafter, the fungi were treated with 100% ethanol thrice, with each

exposure lasting fifteen minutes. Finally, the hyphae were subjected to vacuum drying, coated with gold, and examined through scanning electron microscopy (SEM) using a Hitachi S-4800 instrument [39].

4. Conclusion

Fifty-two kinds of target compounds were synthesized efficiently and concisely up to 96% yield, and their structures were characterized by HRMS, ^{1}H NMR, and ^{13}C NMR. It was discovered that five of the compounds (**A**$_{7}$, **B**$_{13}$, **D**$_{2}$, **D**$_{4}$, and **D**$_{5}$) were unknown.

The target compounds produced different degrees of inhibition against *C. alb.*, among which **A**$_{11}$ had the highest antifungal activity for all tested fungi, and its TAI value was 2.71, which was higher than that of the positive control FLC (TAI = 1.19). The presence of an electron-absorbing group could significantly enhance antifungal activity of the compounds, in comparison to those having an electron-giving group. Particularly, compound series D showed considerably higher antifungal activity than **A**$_{1}$. The IT$_{50}$ values of the seven compounds were about half that of FLC, and **A**$_{11}$ was only 1.4 h, which had a more efficient antifungal mechanism.

Further exploration of mechanisms revealed that **A**$_{11}$ promoted the generation of endogenous ROS and free radicals, disrupted the physiological processes of *C. alb.* SC5314 and impaired its filamentous morphology, ultimately inhibited fungal growth.

In summary, **A**$_{11}$ is expected to be a novel fungicide, and this research held significant importance for the development of antifungal agents. Next, in vivo antifungal activity and cytotoxicity assays will be carried out.

Supplementary Materials: The following supporting information can be downloaded at the website of this paper posted on Preprints.org.

Author Contributions: Conceptualization, Panpan Zhu and Huiling Geng; Data curation, Panpan Zhu; Funding acquisition, Huiling Geng; Investigation, Panpan Zhu; Supervision, Huiling Geng; Writing – original draft, Panpan Zhu, Jinshuo Zheng, Jin Yan, Zhaoxia Li and Xinyi Li; Writing – review & editing, Panpan Zhu, Jinshuo Zheng, Jin Yan, Zhaoxia Li and Xinyi Li.

Funding: This research was funded by the National Natural Science Foundation of China (No. 31572038) and the Key Research and Development Project of Shaanxi Province (2023-YBNY-242).

Institutional Review Board Statement: Not applicable.

Informed Consent Statement: Not applicable.

Data Availability Statement: Not applicable.

Acknowledgments: We extend our sincere appreciation to the Chemical Experiment Teaching and Research Center for their valuable support in conducting nuclear magnetic resonance analysis. Additionally, we are thankful to the Life Science Research Core Service for providing us with access to electron microscopy analysis and ESI-HRMS.

Conflicts of Interest: The authors declare no conflict of interest.

References

1. Marston, H.D.; Dixon, D.M.; Knisely, J.M.; Palmore, T.N.; Fauci, A.S. Antimicrobial Resistance. *JAMA* **2016**, *316*, 1193-1204.
2. Dartois, V.A.; Rubin, E.J. Anti-Tuberculosis Treatment Strategies and Drug Development: Challenges and Priorities. *Nature Reviews Microbiology* **2022**, *20*, 685-701.
3. Zhang, Y.; Li, Q.; Chao, W.; Qin, Y.; Chen, J.; Wang, Y.; Liu, R.; Lv, Q.; Wang, J. Design, Synthesis and Antifungal Evaluation of Novel Pyrylium Salt in Vitro and in Vivo. *Molecules* **2022**, *27*, 4450.
4. Arendrup, M.C.; Patterson, T.F. Multidrug-Resistant Candida: Epidemiology, Molecular Mechanisms, and Treatment. *J Infect Dis* **2017**, *216*, S445-S451.
5. Wijnants, S.; Vreys, J.; Van Dijck, P. Interesting Antifungal Drug Targets in the Central Metabolism of *Candida Albicans*. *Trends in Pharmacological Sciences* **2022**, *43*, 69-79.
6. Nobile, C.J.; Johnson, A.D. *Candida Albicans* Biofilms and Human Disease. *Annu. Rev. Microbiol.* **2015**, *69*, 71-92.

7. Xiao, M.; Sun, Z.Y.; Kang, M.; Guo, D.W.; Liao, K.; Chen, S.C.; Kong, F.; Fan, X.; Cheng, J.W.; Hou, X.; et al. Five-Year National Surveillance of Invasive Candidiasis: Species Distribution and Azole Susceptibility from the China Hospital Invasive Fungal Surveillance Net (Chif-Net) Study. *J Clin Microbiol* **2018**, *56*.
8. Mukaremera, L.; Lee, K.K.; Mora-Montes, H.M.; Gow, N.A.R. *Candida Albicans* Yeast, Pseudohyphal, and Hyphal Morphogenesis Differentially Affects Immune Recognition. *Frontiers in Immunology* **2017**, *8*.
9. Tits, J.; Cammue, B.P.A.; Thevissen, K. Combination Therapy to Treat Fungal Biofilm-Based Infections. *Int. J. Mol. Sci.* **2020**, *21*, 8873.
10. Mahboub, H.H.; Eltanahy, A.; Omran, A.; Mansour, A.T.; Safhi, F.A.; Alwutayd, K.M.; Khamis, T.; Husseiny, W.A.; Ismail, S.H.; Yousefi, M.; et al. Chitosan Nanogel Aqueous Treatment Improved Blood Biochemicals, Antioxidant Capacity, Immune Response, Immune-Related Gene Expression and Infection Resistance of Nile Tilapia. *Comparative Biochemistry and Physiology Part B: Biochemistry and Molecular Biology* **2024**, *269*, 110876.
11. Li, J.; Buchner, J. Structure, Function and Regulation of the Hsp90 Machinery. *Biomed J* **2013**, *36*, 106-117.
12. Lee, K.-H.; Park, S.J.; Choi, S.J.; Park, J.Y. Proteus Vulgaris and Proteus Mirabilis Decrease *Candida Albicans* Biofilm Formation by Suppressing Morphological Transition to Its Hyphal Form. *Yonsei Med. J.* **2017**, *58*, 1135-1143.
13. White, P.L.; Dhillon, R.; Hughes, H.; Wise, M.P.; Backx, M. Covid-19 and Fungal Infection: The Need for a Strategic Approach. *The Lancet Microbe* **2020**, *1*, e196.
14. Maubon, D.; Garnaud, C.; Calandra, T.; Sanglard, D.; Cornet, M. Resistance of Candida Spp. To Antifungal Drugs in the Icu: Where Are We Now? *Intensive Care Medicine* **2014**, *40*, 1241-1255.
15. Hoang, A. Caspofungin Acetate: An Antifungal Agent. *Am. J. Health-Syst. Pharm.* **2001**, *58*, 1206-1214.
16. Richardson, K.; Cooper, K.; Marriott, M.S.; Tarbit, M.H.; Troke, P.F.; Whittle, P.J. Discovery of Fluconazole, a Novel Antifungal Agent. *Rev Infect Dis* **1990**, *12 Suppl 3*, S267-S271.
17. Boken, D.J.; Swindells, S.; Rinaldi, M.G. Fluconazole-Resistant *Candida Albicans*. *Clin Infect Dis* **1993**, *17*, 1018-1021.
18. Pasquale, T.; Tomada, J.R.; Ghannoun, M.; Dipersio, J.; Bonilla, H. Emergence of Candida Tropicalis Resistant to Caspofungin. *J. Antimicrob. Chemother.* **2008**, *61*, 219.
19. Sawant, B.; Khan, T. Recent Advances in Delivery of Antifungal Agents for Therapeutic Management of Candidiasis. *Biomed. Pharmacother.* **2017**, *96*, 1478-1490.
20. Carmo, A.; Rocha, M.; Pereirinha, P.; Tomé, R.; Costa, E. Antifungals: From Pharmacokinetics to Clinical Practice. *Antibiotics* **2023**, *12*, doi:10.3390/antibiotics12050884.
21. Wang, D.; Zetterström, C.E.; Gabrielsen, M.; Beckham, K.S.H.; Tree, J.J.; Macdonald, S.E.; Byron, O.; Mitchell, T.J.; Gally, D.L.; Herzyk, P.; et al. Identification of Bacterial Target Proteins for the Salicylidene Acylhydrazide Class of Virulence-Blocking Compounds*. *Journal of Biological Chemistry* **2011**, *286*, 29922-29931.
22. Tirapegui, C.; Acevedo-Fuentes, W.; Dahech, P.; Torrent, C.; Barrias, P.; Rojas-Poblete, M.; Mascayano, C. Easy and Rapid Preparation of Benzoylhydrazides and Their Diazene Derivatives as Inhibitors of 15-Lipoxygenase. *Bioorganic & Medicinal Chemistry Letters* **2017**, *27*, 1649-1653.
23. Kozlov, M.V.; Konduktorov, K.A.; Shcherbakova, A.S.; Kochetkov, S.N. Synthesis of N′-Propylhydrazide Analogs of Hydroxamic Inhibitors of Histone Deacetylases (Hdacs) and Evaluation of Their Impact on Activities of Hdacs and Replication of Hepatitis C Virus (Hcv). *Bioorganic & Medicinal Chemistry Letters* **2019**, *29*, 2369-2374.
24. Turan-Zitouni, G.; Altintop, M.D.; Ozdemir, A.; Demirci, F.; Abu Mohsen, U.; Kaplancikli, Z.A. Synthesis and Antifungal Activity of New Hydrazide Derivatives. *J Enzyme Inhib Med Chem* **2013**, *28*, 1211-1216.
25. Pham, V.H.; Phan, T.P.D.; Phan, D.C.; Vu, B.D. Synthesis and Bioactivity of Hydrazide-Hydrazones with the 1-Adamantyl-Carbonyl Moiety. *Molecules* **2019**, *24*.
26. Nam, G.; Suh, J.-M.; Yi, Y.; Lim, M.H. Drug Repurposing: Small Molecules against Cu(Ii)–Amyloid-B and Free Radicals. *Journal of Inorganic Biochemistry* **2021**, *224*, 111592.
27. Ganrot, P.O.; Rosengren, E.; Gottfries, C.G. Effect of Iproniazid on Monoamines and Monamine Oxidase in Human Brain. *Experientia* **1962**, *18*, 260-261.
28. Zhang, H.-Z.; Drewe, J.; Tseng, B.; Kasibhatla, S.; Cai, S.X. Discovery and Sar of Indole-2-Carboxylic Acid Benzylidene-Hydrazides as a New Series of Potent Apoptosis Inducers Using a Cell-Based Hts Assay. *Bioorganic & Medicinal Chemistry* **2004**, *12*, 3649-3655.

29. Wu, Y.-Y.; Shao, W.-B.; Zhu, J.-J.; Long, Z.-Q.; Liu, L.-W.; Wang, P.-Y.; Li, Z.; Yang, S. Novel 1,3,4-Oxadiazole-2-Carbohydrazides as Prospective Agricultural Antifungal Agents Potentially Targeting Succinate Dehydrogenase. *Journal of Agricultural and Food Chemistry* **2019**, *67*, 13892-13903.
30. Clements, J.S.; Islam, R.; Sun, B.; Tong, F.; Gross, A.D.; Bloomquist, J.R.; Carlier, P.R. N′-Mono- and N, N′-Diacyl Derivatives of Benzyl and Arylhydrazines as Contact Insecticides against Adult Anopheles Gambiae. *Pesticide Biochemistry and Physiology* **2017**, *143*, 33-38.
31. de Sousa, E.S.O.; Cortez, A.C.A.; de Souza Carvalho Melhem, M.; Frickmann, H.; de Souza, J.V.B. Factors Influencing Susceptibility Testing of Antifungal Drugs: A Critical Review of Document M27-A4 from the Clinical and Laboratory Standards Institute (Clsi). *Brazilian Journal of Microbiology* **2020**, *51*, 1791-1800.
32. Yang, S.-S.; Lv, Q.-Y.; Fu, J.; Zhang, T.-Y.; Du, Y.-S.; Yang, X.-J.; Zhou, L. New 7-Chloro-9-Methyl-2-Phenyl-3,4-Dihydro-B-Carbolin-2-Iums as Promising Fungicide Candidates: Design, Synthesis, and Bioactivity. *Journal of Agricultural and Food Chemistry* **2022**, *70*, 4256-4266.
33. Kalgutkar, A.S.; Gardner, I.; Obach, R.S.; Shaffer, C.L.; Callegari, E.; Henne, K.R.; Mutlib, A.E.; Dalvie, D.K.; Lee, J.S.; Nakai, Y.; et al. A Comprehensive Listing of Bioactivation Pathways of Organic Functional Groups. *Curr Drug Metab* **2005**, *6*, 161-225.
34. Kakizaki, T.; Abe, H.; Kotouge, Y.; Matsubuchi, M.; Sugou, M.; Honma, C.; Tsukuta, K.; Satoh, S.; Shioya, T.; Nakamura, H.; et al. Live-Cell Imaging of Septins and Cell Polarity Proteins in the Growing Dikaryotic Vegetative Hypha of the Model Mushroom Coprinopsis Cinerea. *Scientific Reports* **2023**, *13*, 10132.
35. Triastuti, A.; Vansteelandt, M.; Barakat, F.; Amasifuen, C.; Jargeat, P.; Haddad, M. Untargeted Metabolomics to Evaluate Antifungal Mechanism: A Study of Cophinforma Mamane and *Candida Albicans* Interaction. *Natural Products and Bioprospecting* **2023**, *13*, 1.
36. Zhang, Y.-H.; Yang, S.-S.; Zhang, Q.; Zhang, T.-T.; Zhang, T.-Y.; Zhou, B.-H.; Zhou, L. Discovery of N-Phenylpropiolamide as a Novel Succinate Dehydrogenase Inhibitor Scaffold with Broad-Spectrum Antifungal Activity on Phytopathogenic Fungi. *Journal of Agricultural and Food Chemistry* **2023**, *71*, 3681-3693.
37. Jacob, N.; Guillemard, L.; Wencel-Delord, J. Highly Efficient Synthesis of Hindered 3-Azoindoles Via Metal-Free C-H Functionalization of Indoles. *Synthesis* **2020**, *52*, 574-580.
38. Afri, M.; Frimer, A.A.; Cohen, Y. Active Oxygen Chemistry within the Liposomal Bilayer Part Iv: Locating 2',7'-Dichlorofluorescein (Dcf), 2',7'-Dichlorodihydrofluorescein (Dcfh) and 2',7'-Dichlorodihydrofluorescein Diacetate (Dcfh-Da) in the Lipid Bilayer. *Chem. Phys. Lipids* **2004**, *131*, 123-133.
39. Wang, D.; Zhang, J.; Jia, X.; Xin, L.; Zhai, H. Antifungal Effects and Potential Mechanism of Essential Oils on Collelotrichum Gloeosporioides in Vitro and in Vivo. *Molecules* **2019**, *24*, doi:10.3390/molecules24183386.